Term 2 Coursework: Influence Lines and Bridge Structure

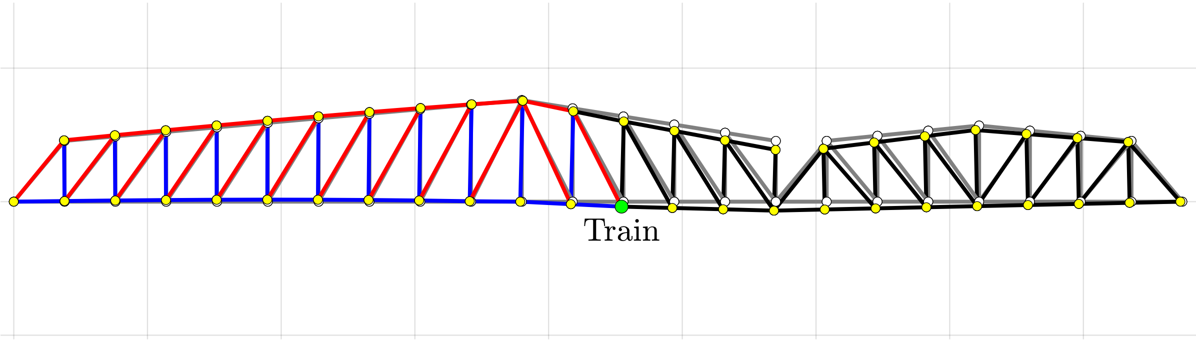

Majd Yousof

CIVE50003 Computational Methods II

1. Introduction

This report is an investigation into the static behaviour of a truss bridge using the influence lines of reactions and axial forces of chord members. This is represented using a point load with a magnitude of 2 MN which travels the bottom nodes of the bridge; this emulates a simplification of a train traversing the bridge. To solve this numerically, a bespoke bridge class was created to allow for 2D finite element analysis. Every figure in this report is vectorised, so feel free to zoom in as much as you want.

2. Influence lines: Hand Calculations

*This section aims to answer **Q1** and **Q2**.*

To calculate the influence lines of the reactions at A, B, C, and the force exerted at point D, the truss bridge is to be assumed as a determinate system, consisting of simply supported and cantilever beams. This is achieved through 2 layers of abstraction, first assuming that the entire bridge can be represented as a beam with 2 hinges at points C and D. This can be further idealised into 3 independent determinate beam systems, and it can be assumed that C and D can be represented as a pinned joint and a roller joint respectively, and the force at D as a reaction force. A diagram demonstrating this can be found in the coursework brief (*Sadowski, 2023*).

Due to these assumptions as well as the train being represented as a 2 MN point load, it is clear that the influence lines will be linear in this case, so it is possible to calculate them from interpolating the reactions at each point for each of the reaction forces (R_A, R_B and R_D). R_D will only be plotted until point D as the question specifies.

2.1. Hand calculation plotting

Table 2.1.1: Reaction Force values per location

	A	B	C	D	E	F
R_A [MN]	2	0	-1	0	0	0
R_B [MN]	0	2	3	0	0	0
R_D [MN]	0	0	0	2		

The values that were calculated in table 2.1.1 are then used to plot figure 2.1.1 shown below, which is the plot required for ***Q1:***

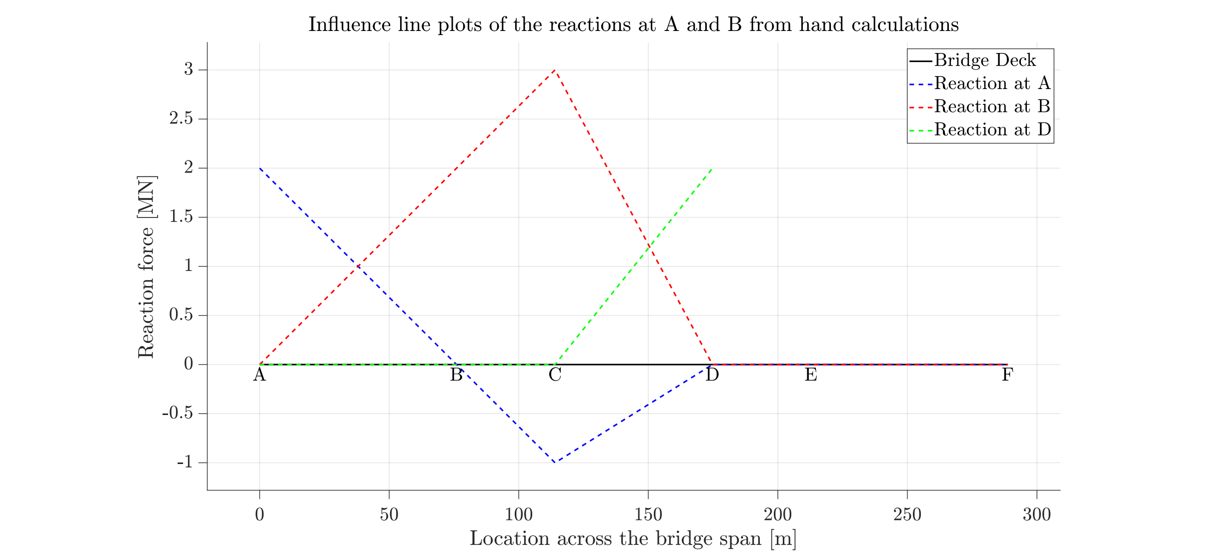

Figure 2.1.1: Hand-calculated values for the influence lines

2.2 Justifications for reduced model

As can be seen in figure 2.1.1, after the train load passes point D, the influence lines of the reactions at A and B are consistently zero, implying that they have no effect on the load distribution past that point. This then would ultimately save us computational time, through calculation and also the time it takes to write and run the code. As well as that, the bridge is symmetrical, which allows us to ensure that we can run use our reduced model to calculate the values for the entire bridge conveniently.

3. Influence Lines: Finite Element Analysis

*This section aims to answer **Q3**, **Q5**, **Q6**, **Q7**, and **Q8**.*

Through FEA conducted in MATLAB using a bespoke BRIDGE class for the specified region (points A-D), we are able to obtain the influence lines for the reactions and axial forces across certain members as mentioned before. This includes plots with and without the addition of the extra member O1-O2 to the truss bridge. Before the influence line plots are presented, it is important to discuss the methods that were decided upon to produce the results.

3.1. Cholesky Decomposition

To introduce the concept, Cholesky decomposition provides a means for a positive, definite symmetrical (or Hermitian, but in this case, it is symmetric) matrix to be factorised into a lower triangular matrix multiplied by its transpose (Lindfield & Penny, 2019). This principle was used particularly to decompose the matrix $\mathbf{k_{FF}}$ within the solver module in the BRIDGE class created:

$$\boldsymbol{k_{FF}} = \boldsymbol{P} \times \boldsymbol{P^T}$$

Where P is the lower triangular matrix. In MATLAB, the specific matrix inversions that can be conducted to solve the global stiffness matrix in context to the BRIDGE class are:

- `obj.k.kFF\dFequation;` - Regular matrix inversion.
- `cholkFF\(cholkFF'\dFequation);` - Matrix inversion using Cholesky matrix.

To see which method is most efficient for the use case, 3 factors were considered to assess the performance of each method. For this, we set the train load on a random location on the bridge span (shown in figure 3.1.2) and repeated the calculations for **10,000 iterations** (all of the test parameters can be altered within the plot file included with this report):

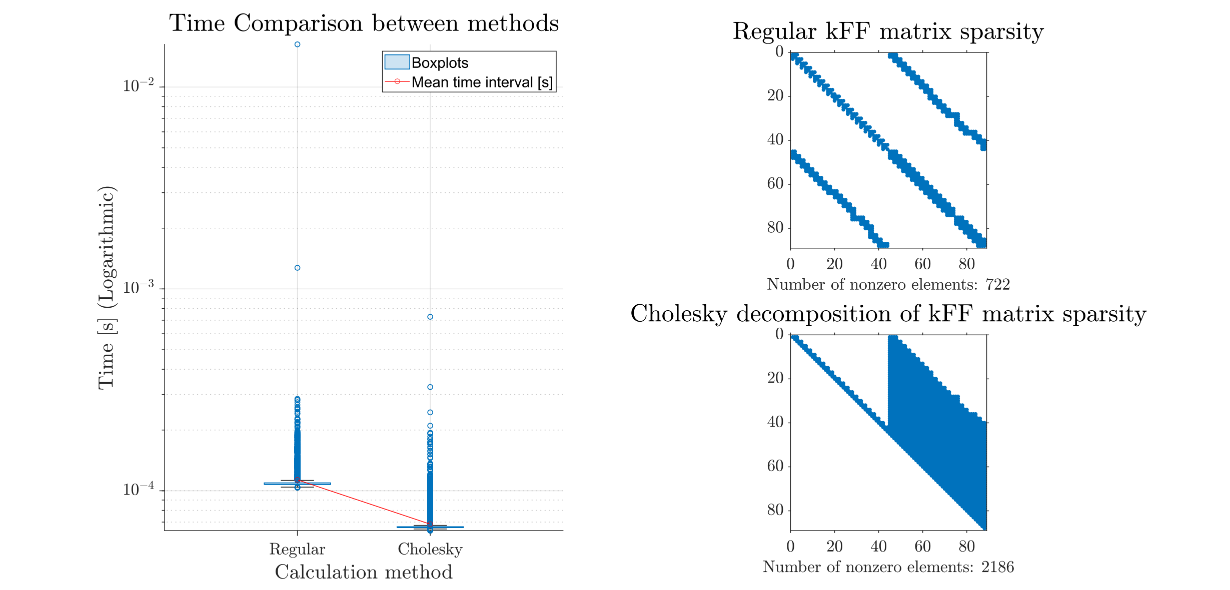

Figure 3.1.1: Cholesky decomposition comparisons for specific train location

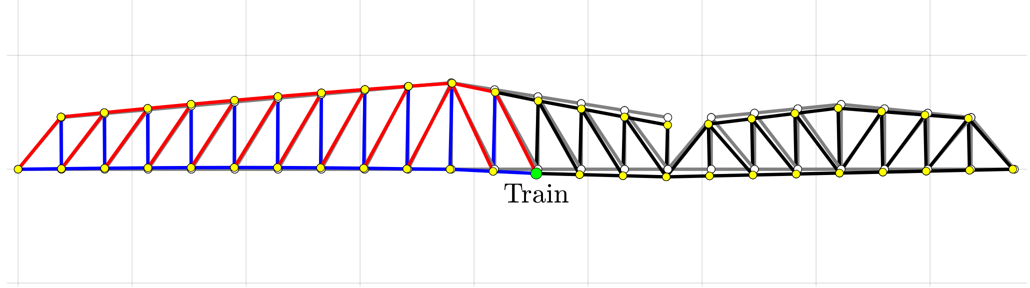

Figure 3.1.2: Truss deformation for Cholesky decomposition comparison

As shown in figure 3.1.1, on average the time it takes for the matrix inversion using the Cholesky decomposition method is less than the regular method, having taken mean times of 7.0×10^{-5} seconds and 1.1×10^{-4} seconds respectively - one thing to note is that the time it takes to execute MATLAB's *chol* function is also included in the Cholesky method timing. It can also be seen that the matrix sparsity of the Cholesky matrix is much lower than that of the original $\mathbf{k_{FF}}$ matrix, which makes it easier to inverse. Additionally, the reciprocal condition value (*rcond*) of the Cholesky matrix is 1.4×10^{-3} compared to 7.5×10^{-5} for $\mathbf{k_{FF}}$**,** which indicates that the Cholesky matrix is much better conditioned than $\mathbf{k_{FF}}$. From these results one can definitely see the benefits of Cholesky decomposition for this application.

3.2. Plots: Influence lines without O1-O2

3.2.1. Influence line plots

In figure 3.2.1 below, it is clear that the hand calculated values are identical to the ones calculated computationally for the influence lines of the specified reactions.

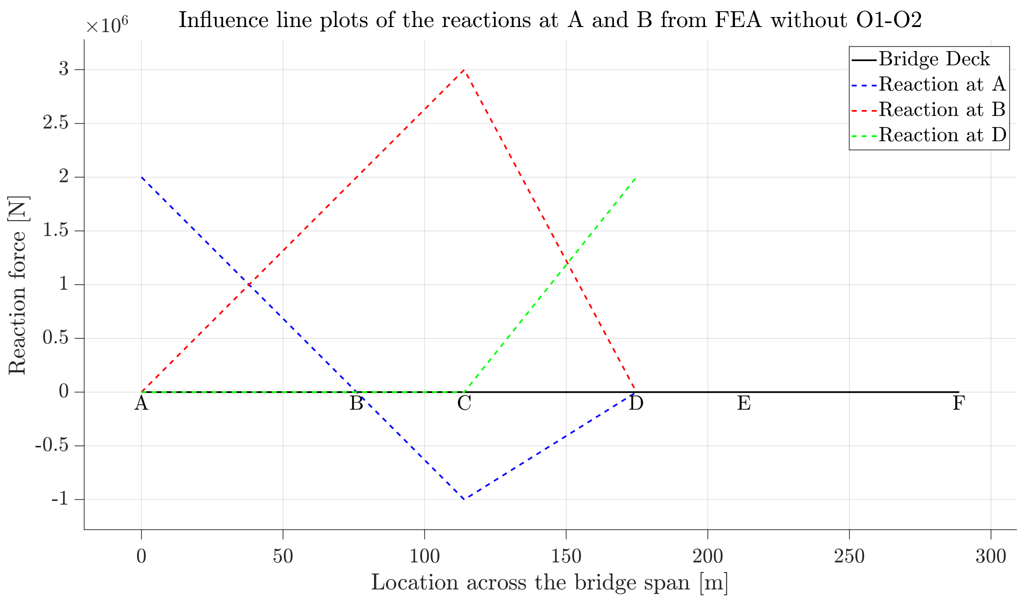

Figure 3.2.1.1: Influence line plot for A, B, and D

The reason we model D as a roller is because the hinge will always exert an equal and opposite reaction on the 2 separate parts of the bridge. As well as that, if a support is not present at point D, the system will turn into a mechanism, as the statical determinacy will be negative, and there will be no force keeping the hinge at C from rotating, as it does not transfer moment.

In figure 3.2.2 and 3.2.3, we can see the influence lines for the axial force distributions from members B1-B10 and T1 to T10 respectively.

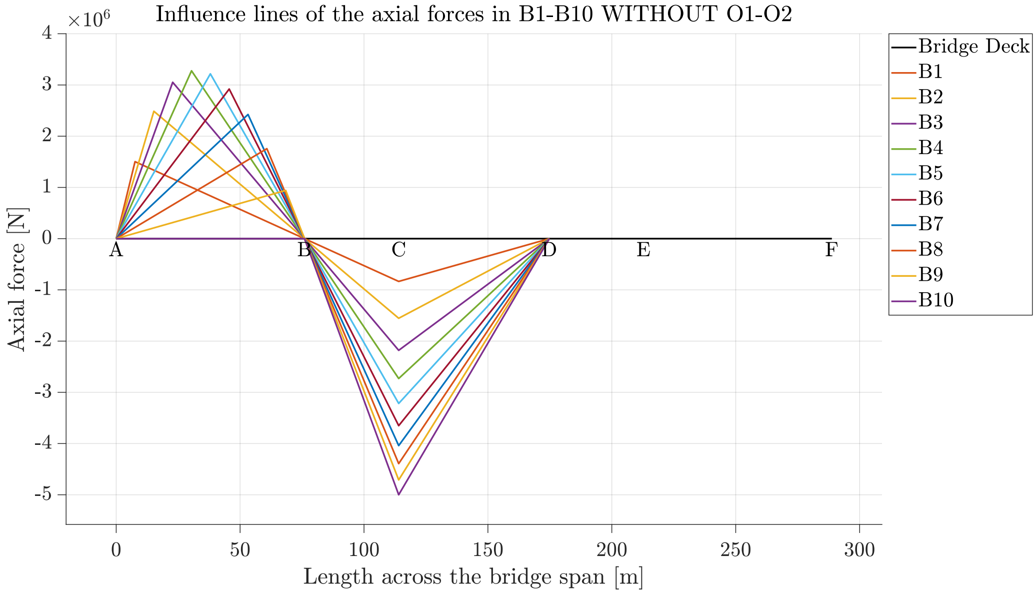

Figure 3.2.1.2 Influence line plots for B1-B10 using FEA

As can be seen in figure 3.2.2 above, as the train passes through between A and B, the bottom chords of the anchor arm all experience a tensile axial force except for B10. The tensile peaks for each element tend to be when the point load is present at the end/second node of the element. The highest tensile axial force was experienced by **B4**, with a value of **3.28 MN**. This is to be expected as the location of B4's second node is the closest to the centre of A-B, which is where the highest value of deflection occurs in a simply supported beam subjected to a point load at its centre. This is exactly how we have abstracted this portion in previous sections.

As the train moves to the portion between B and D (figure 3.3.1.2), all elements are in compression, and all have peaks when the train load is at point C. The highest value of compressive axial force was experienced by **B10**, with a value of **-5.00 MN**. The absolute maximum axial force for the entire plot was at **point C by B10**.

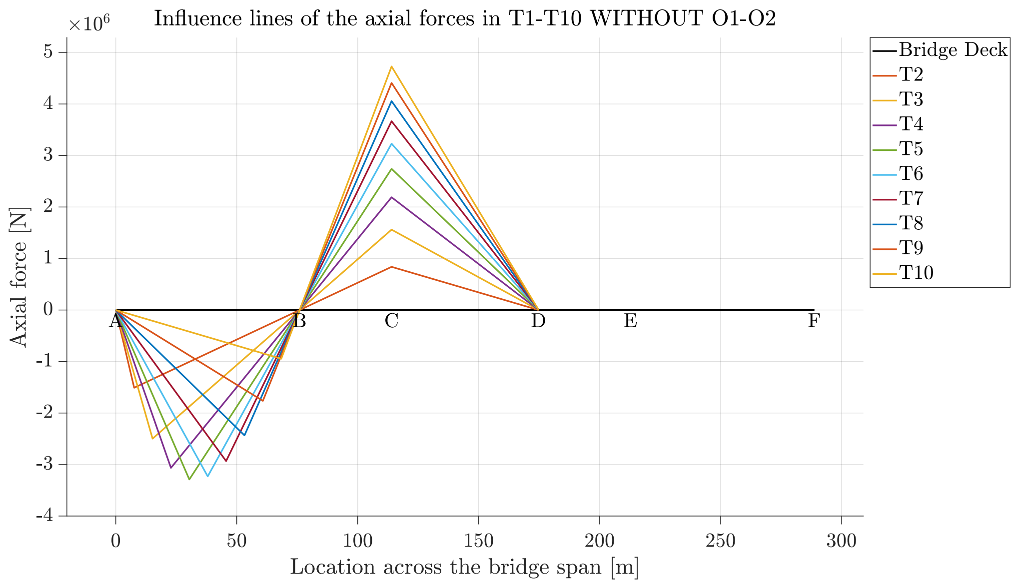

Figure 3.2.1.3 Influence line plots for T2-T10 using FEA

From what can be seen in figure 3.2.3 for T2-T10, the influence lines are a mirror image reflected on the x-axis of the influence lines of B1-B9 (where *B1=-T2*, *B2=-T3*, etc.). The element that experienced the highest compressive axial force was **T5** with a value of **-3.29 MN**, and as for the highest tensile axial force, it was being experienced by **T10** with a value of **4.73 MN**. The absolute maximum axial force for the entire plot was experienced over **point C by T10**, in a similar fashion to B10. This symmetry between the influence lines for B1-B10 and T2-T10 can be explained through the abstractions to the model made earlier to complete the hand calculations; the truss bridge was represented as a beam subjected to a point load acting downwards.

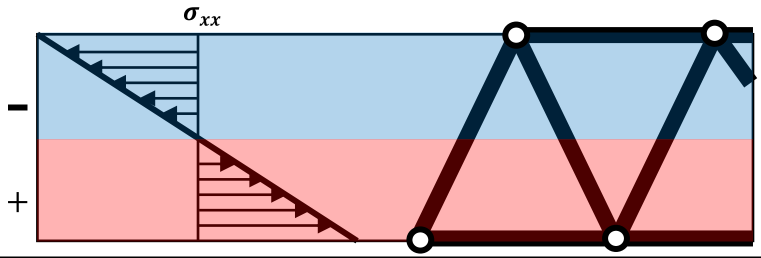

Figure 3.2.1.4: Beam abstraction of truss bridge visualised (train between A-B particularly)

As shown in figure 3.2.4, as the truss is abstracted as a solid beam and when section A-B is subjected to the train point load, the upper most fibres experience the most compression whilst the lowermost fibres experience the most tension; both compression and tension are of equal magnitude. This behaviour was shown to be true in the truss bridge model due to the symmetry of the influence lines, where the upper most fibres represent elements T2-T10, and the lowermost fibres representing elements B1-B10. The figure is only accurate when the load is located within the span of A-B, however the same principle can also be applied when the load is present outside of this range. From this, we can see that the anchor arm A-B behaves like a solid beam and can be abstracted as such.

3.2.2. Safety factor

For B1-B10 and T2-T10

The minimum safety factor achieved with respect to Euler buckling was **0.67**, achieved by **B10** when the load is at **point C.** For the safety factor governed by plastic collapse, the lowest value was **1.51**, achieved by **B10**, when the train load was at **point C**. This indicates that these chords are not safe enough for the bridge, with the critical element being **B10**.

For the global truss

As the train traverses the truss bridge, it is found that the lowest safety factor achieved through Euler's buckling load (**P_{cr}**) in the entire structure is **0.28**, experienced by **element 33** when the train is at **point C** (**location 16**). The safety factor for plastic collapse (**P_s**) is controlled by **element 10** (**B10**), with a value of **1.51** when the load is at **point C** (**location 16**). The worst location for the train to be in is at point C, which makes sense due to it not being able to transfer moment as it is a hinge, as shown in figure 3.2.2.1.

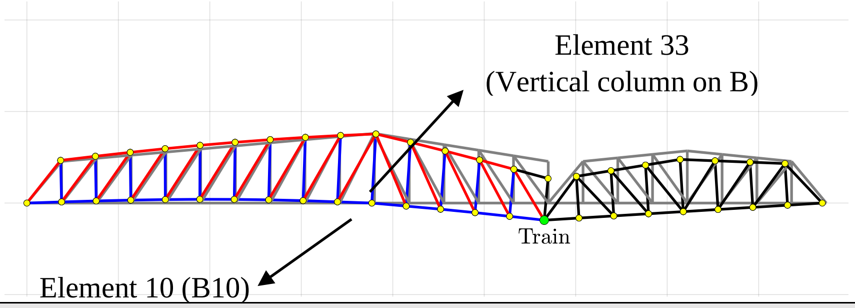

Figure 3.2.2.1: Critical load location and elements

If we take it as the minimum safety factor for the bridge not to fail is equal to 1, we begin to see that certain elements begin to fail through buckling much earlier than what is presented in figure 3.2.2.1. That is because a value below 1 implies that the compressive axial load is higher than the critical load of the element, which indicates failure. As soon as the train passes location 2 (right after A) **element 46** achieves a safety factor (using P_{cr}) of **0.59**, indicating that it has buckled.

3.3. Plots: Influence lines with O1-O2 added

3.3.1. Influence line plots

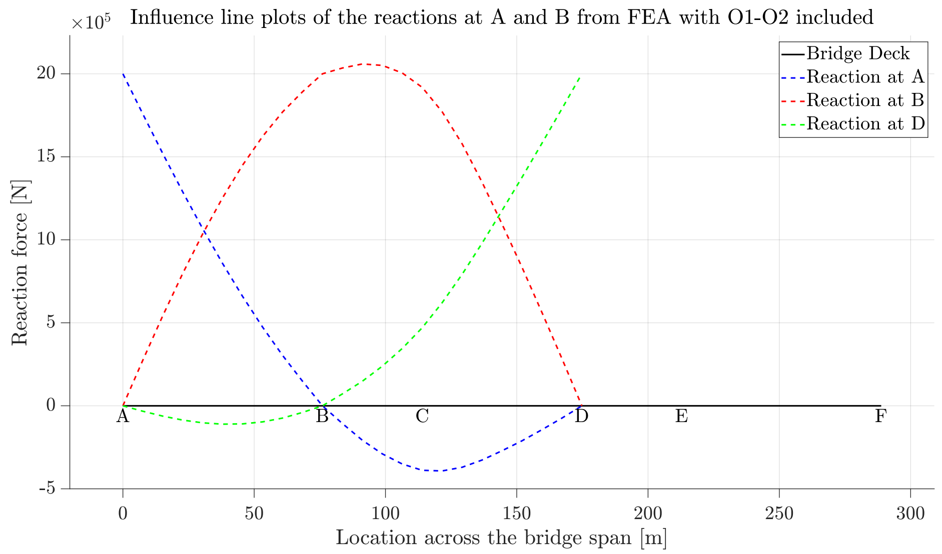

Figure 3.3.1: Influence line plot for A, B, and D with O1-O2

Figure 3.3.1 showcases the influence lines for the reactions when the element O1-O2 is added. Unlike the plot for the truss bridge without O1-O2, the influence lines aren't linear but rather polynomial-like, although they take a similar shape. The maximum magnitude of reaction force was experienced by $\mathbf{R_A}$, with a value of **2.06 MN**, contrary to the truss bridge without O1-O2, where the maximum magnitude of reaction force experienced was **3.00 MN** by $\mathbf{R_A}$. This implies that the train load was distributed more evenly overall, which can be seen when running the animation in `plotfile.m` that comes with this report, and also figure 3.3.2 below.

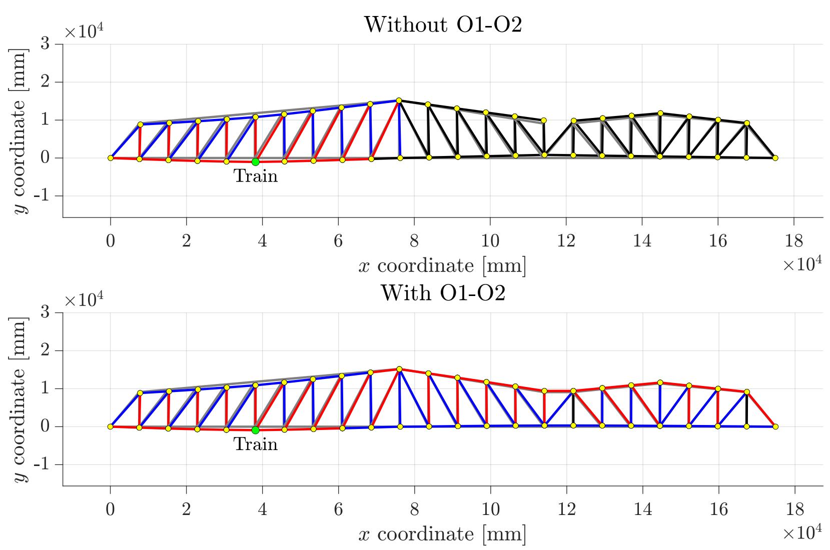

Figure 3.3.2: Comparison of force distribution in the two different truss bridges

It can be clearly seen that the truss with O1-O2 engages more elements with the load as the hinge is completely eliminated, and the structure can now transmit moments through point C.

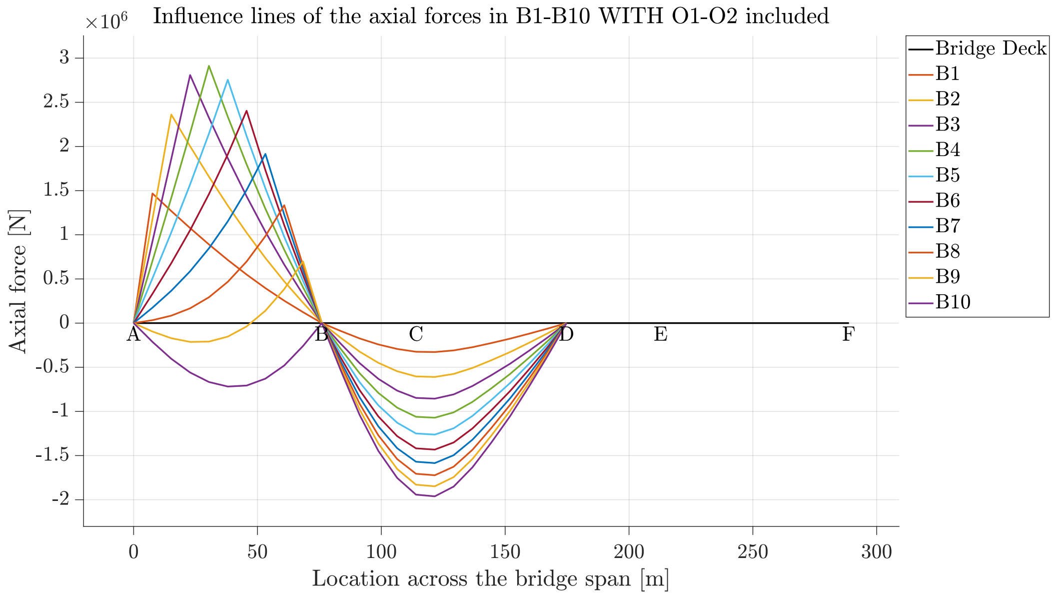

Figure 3.3.1.2 Influence line plots for B1-B10 using FEA with O1-O2 included

As seen in figure 3.3.1.2, the figure is very similar to the plot for B1-B10 for the previous truss structure without O1-O2, although rather than linear, the graphs are broadly take on a polynomial shape. Broadly, the same arguments can be made for the loading of the axial loading of this truss and the original, with the exception of having a hinge. The maximum compressive force was experienced by **B10**, with a value of **-1.96 MN.** it is the same element as the previous truss bridge but has a load that is 39.2% of the axial load in the previous truss. This is the same story with the maximum axial tension, which was experienced by B4, with a value of **2.91 MN** which is 88,7% of the original axial load. This was due to the more even distribution of loading.

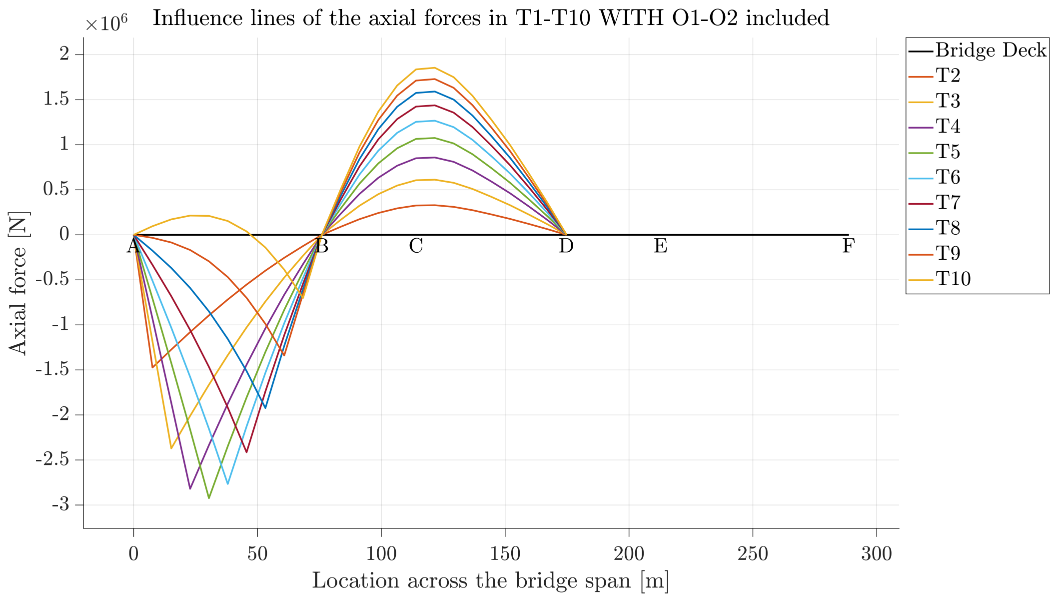

Figure 3.3.1.3 Influence line plots for T2-T10 using FEA with O1-O2 included

Again, similarly to the original influence lines, the plot of T2-T10 is a mirror image of B1-B9. The highest compressive axial force achieved was **1.85 MN** by T10, and the highest overall compressive axial force was **2.92 MN**, achieved by **T5**. The members are the same as the original truss bridge, however, the values calculated were significantly lower. From this we can really see the impact on loading adding 1 extra element can be, especially as it allows the moment to be transferred across the structure by getting rid of the hinge.

3.3.2. Safety Factor

For B1-B10 and T2-T10

When only taking the top and bottom chords in A-B into consideration, we find that the minimum buckling safety factor is **1.14** which is achieved by **T5** when the train is at load **location 5**. The minimum for the Safety factor derived with plastic collapse has a value of **2.58**, achieved by **T5** at load **location 5**. Both values being above 1 indicates that the top and bottom chords are resistant to failure, unlike with the original bridge truss.

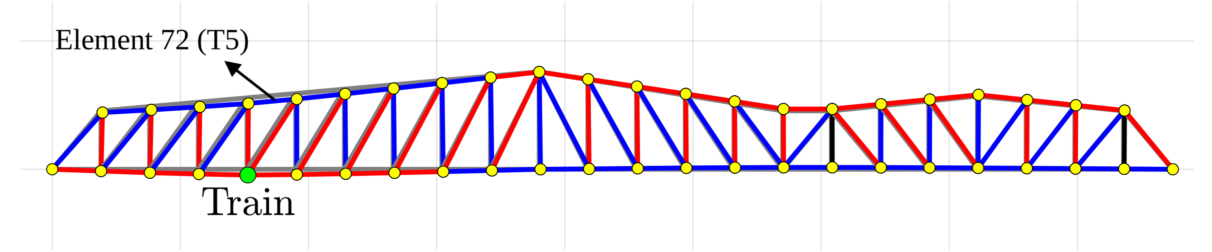

Figure 3.3.2.1: P_{cr} load location and element and P_s load location and element

For the global truss

The lowest value of safety factor calculated according to Euler buckling load (**P_{cr}**) as the train traverses the bridge truss is **0.41**, governed by **element 33** (**vertical column at point B**) when the load is at **location 13** (**directly after the train passes point B**). On the other hand, the minimum safety factor according to plastic collapse (**P_s**) is **2.05**, controlled by **element 83**, when the train is at **location 18** (**directly after the train passes point C**). As can be seen from the values calculated, compared to the previous truss, the safety values have increased, which imply the bridge is safer to for the train to cross, although the lowest value of safety factor is still well below 1 (Euler's buckling safety factor). As this is the case, the compressive axial force is more than double the Euler buckling load of element 33, which means that its very likely that this element will fail through buckling. In fact, as soon as the train passes over point 2 (right after A), **element 46** reaches a safety factor of only 0.61, implying the bridge fails very early on just as the previous truss bridge has (assuming the minimum safety factor before collapse is equal to 1). This is the exact same element as the previous bridge truss, although the safety factor value is higher.

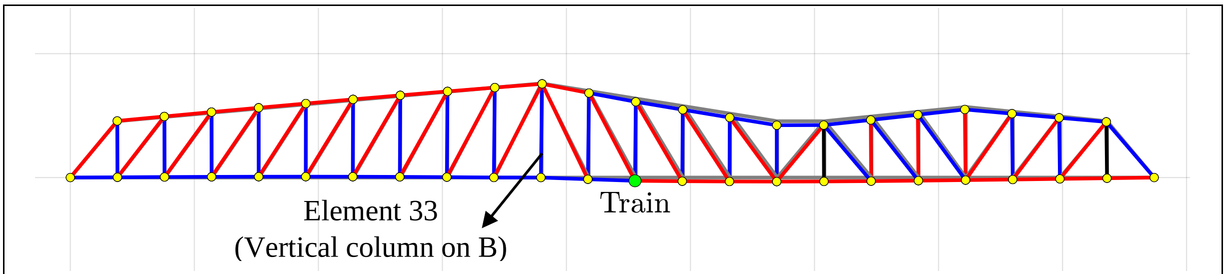

Figure 3.3.2.2: P_{cr} load location and element

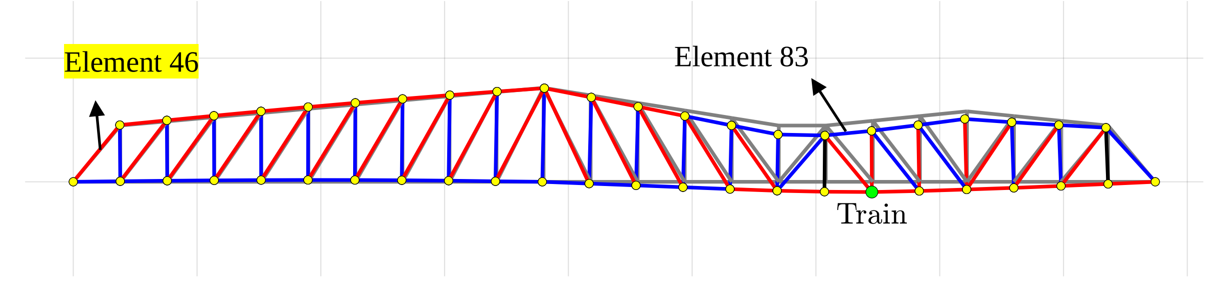

Figure 3.3.2.3: P_s load location and element

4. Statical determinacy

*This section aims to answer **Q4**.*

4.1. Structural arguments

For truss structures, the static indeterminacy/redundancy helps identify whether a structure is determinate, indeterminate or a mechanism. Specifically for trusses, it is calculated using this specific equation:

$$\boldsymbol{E + R - 2 * N}$$

Where E is the number of elements in the truss, R is the number of reactions and N is the number of nodes present within the structure. If this value is above 0, the truss is statically indeterminate, if it is equal to 0, it is statically determinate and if it is below 0, the truss is a mechanism. Before removing any diagonal nodes, the statical redundancy of the truss is equal to:

$$\mathbf{88 + 4 - (2 * 46) = 0}$$

This indicates that the structure is **statically determinate**. However once one of the elements is removed, that value then drops to **-1**. So regardless of what element is removed, the statical redundancy indicates that it will **cause the system to become a mechanism** rather than a structure, which is not ideal in this use case.

4.2. Computational arguments

The structural calculation executed computationally is heavily reliant on the inversion of the k matrix. Once 1 element is removed, that then affects the k matrix calculated in the assembler module, which changes the values of the diagonal. These changes cause the k matrix to then to have a determinant of 0 or a value very close to that, which implies that the matrix is **singular**. To test this, 1 diagonal element was removed from the structure with the load situated at location 2 and the code was run to produce figure 4.2.1 (available in the next page).

It was also found that the k matrix produced for this plot achieved a reciprocal condition value (*rcond*) of $\mathbf{7.8\times10^{-19}}$, which indicates that k is an extremely poorly conditioned matrix. From the plot and the reciprocal condition value, it was quite clear that the model was producing incorrect and unusable results. These factors indicate that the truss system was not statically determinate or indeterminate and was in fact a mechanism.

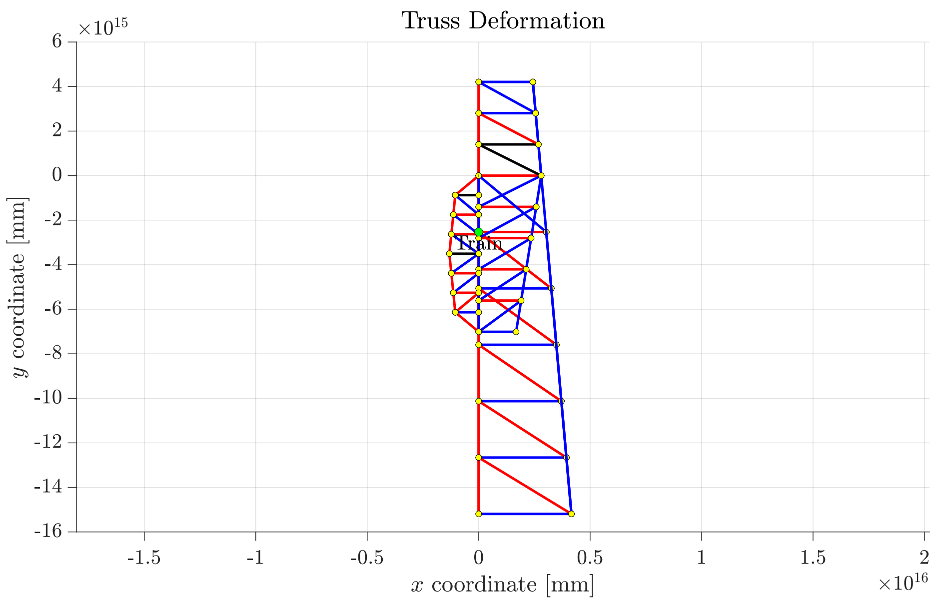

Figure 4.2.1 Structural calculation without diagonal element

References

Sadowski, A. (2023). *Coursework – Influence lines and bridge structures*, CIVE50003 Computational Methods II. Imperial College London. Available from: Blackboard Learn.

Lindfield, G. & Penny, J. (2019). *Linear Equations and Eigensystems*, Numerical Methods using MATLAB®. London, United Kingdom, Academic Press, an imprint of Elsevier. https://doi.org/10.1016/B978-0-12-812256-3.00011-7